ON DEPENDENCE OF THE MULTIJUNCTION InGaP/GaAs/Ge, InGaP/GaAs SOLAR CELL EFFICIENCY ON THE SUNLIGHT CONCENTRATION.

V.S. Kalinovsky, V.V. Evstropov, V.M. Lantratov, M.A. Mintairov, P.V. Pokrovskiy
Ioffe Physico-Technical Institute of RAS
26 Politekhnicheskaya str., Saint Petersburg, 194021, Russia, tel: (812) 2927933, fax: (812) 2971017,
E-mail: vitak.sopt@mail.ioffe.ru

ABSTRACT: Correlation between two main characteristics of multijunction (MJ) solar cells (SC) and their segment character have been studied theoretically and experimentally: the dark voltage – current characteristic and the characteristic corresponding to it: efficiency – concentration ratio, $\eta - C(\propto J_g)$. The characteristics have been investigated in two steps. At the first step, an idealization has been done, which did not take into account of tunnel p^{++} - n^{++} junctions, series resistance of the structure, and other elements. The idealized characteristics have the shape of an uninterrupted function comprised of specific segments. For each segment, an analytical formula expressing the generated current through the efficiency has been derived. The formula derivation has been done at the condition of generated current matching (equality of generated currents in photovoltaic junctions of a MJSC). The analytical $\eta - C(\propto J_g)$ characteristic segment is set by the same two parameters (preexponential factor J_0 and diode coefficient A) as of the corresponding dark V - J characteristic segment. Therefore, the performance connectorless $\eta - C(\propto J_g)$ characteristic is unambiguously associated with the initial connectorless dark V - J characteristic. At the second step, the effect of the MJSC connecting part has been taken into account, which was simulated by selected ohmic resistance. The connectorless $\eta - C(\propto J_g)$ characteristic have been calculated and plotted segment by segment. A good fit between the rated and experimental $\eta - C(\propto J_g)$ dependencies have been obtained for dual-junction InGaP/GaAs SCs. A acceptable fit between the calculated and experimental data has been obtained for triple-junction InGaP/GaAs/Ge SCs, in spite of there is no generated current matching.
Keywords: Solar Cell Efficiencies, Multijunction Solar Cell, Tandem, Concentrator Cells, Gallium Arsenide Based cells.

1 INTRODUCTION

The dependence efficiency (η) of solar cells (SCs) on the sunlight concentration ratio (C) has a maximum [1,2,3].

It has been shown [3] that, on the portion preceding the maximum, quite important are: first, the recombination mechanism (Sah, Noyce, Shockley), second pure-tunneling mechanism and thermo-tunneling (excess by the Esaki terminology [4,5] defect-dependent mechanism. The effect of the excess (tunneling) mechanism rises in decreasing the illuminance, and, in some cases, it becomes rather noticeable at non-concentrated ($C = 1$) and weakened ($C < 1$) solar illumination.

The subject of the present work is the dark *J-V* characteristics of the MJSC photovoltaic (generator) part (Fig.1). The photovoltaic (generator) part means an equivalent circuit containing only photovoltaic *p-n* junctions connected in series. Correspondingly, the connecting part of the MJSC is an equivalent circuit containing tunnel junctions, series resistance, etc (Fig. 1).

The main characteristic practically important for solar cells is the sunlight concentration ratio vs efficiency (C - η). It is derived just from the initial $(J - V)_\varphi$ characteristic [3]. Correspondingly, the $C - \eta$ characteristic shape depends on that the initial $(J - V)_\varphi$ characteristic, which is determined by the current passage mechanism in the SC photovoltaic *p-n* junctions.

The multijunction structures for triple-junction InGaP/Ga(In)As/Ge and dual-junction InGaP/Ga(In)As solar cells have been fabricated by the MOCVD technique.

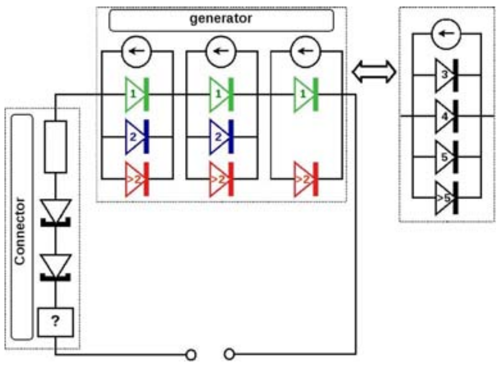

Figure 1: Principal electric equivalent circuit of a triple-junction solar cell consisting of generating (photovoltaic) and connecting (connector) parts.

2 MAIN CHARACTERISTICS OF A MULTIJUNCTION SOLAR CELL.

2.1 Dark and light connectorless current-voltage characteristics of a separate photovoltaic *p-n* junction.

2.1.1. Segment approximation of the dark connectorless current-voltage characteristic.

The dark forward current-voltage characteristic $(J - V)_\varphi$ of each photovoltaic (PV) *p-n* junction comprising a MJSC can be describes by a sum of three current components [6]: diffusion one (the diode coefficient $A_d = 1$), recombination one ($A_r = 2$) and tunneling (defect-dependent) one ($A_t > 2$):

$$J = J_{0t}\left(\exp(\frac{qV_\varphi}{A_t kT})-1\right)+J_{0r}\left(\exp(\frac{qV_\varphi}{A_r kT})-1\right)+J_{0d}\left(\exp(\frac{qV_\varphi}{A_d kT})-1\right) \quad (1)$$

where V_φ is a voltage on the space charge region (SCR) of a photovoltaic *p-n* junction equivalent to the difference between Fermi quasilevels on the boundaries and inside the SCR, J_{0t}, J_{0r}, J_{0d} are corresponding preexponential factors, q is the electron charge, k is the Boltzmann constant, T is the absolute temperature.

The dark $(J - V)_\varphi$ characteristic (1) can be approximated by 3 segments, the SCR voltage on each which is expressed by (Fig.2):

$$V_\varphi = \frac{AkT}{q}\cdot\ln\left(\frac{J}{J_0}+1\right) \quad (2)$$

At such a segment approximation, the whole $(J - V)_\varphi$ characteristic is an uninterrupted function comprised of separate segments. At $V_\varphi > \frac{AkT}{q}$ or $J >> J_0$, one may neglect unity in the brackets of (1) and (2) expressions. Then, the voltage boundary between segments is:

$$V_{ik} = 2\frac{kT}{q}\ln\frac{J_{oi}}{J_{0k}} \quad (3a)$$

where *i, k* are indices of neighboring segments. The current boundary:

$$J_{ik} = \frac{J_{0i}^{A_i/(A_i-A_k)}}{J_{0k}^{A_k/(A_i-A_k)}} \quad (3b)$$

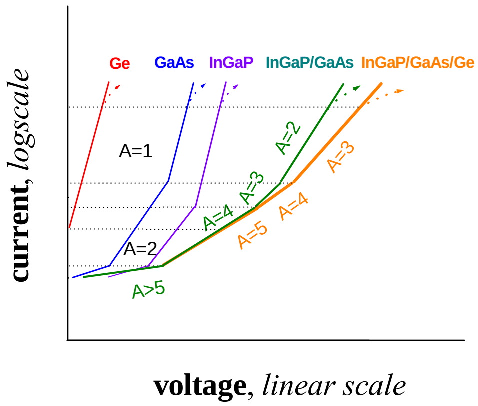

Figure 2: Segmental shape of dark current-voltage characteristic of photovoltaic *p-n* junctions being a part of a multijunction SC. Segmental shape of dark current-voltage characteristic of dual-junction and triple-junction SCs consisting of the *p-n* junctions.

In particular, for the recombination-diffusion boundary:

$$J_{rd} = \frac{J_{0r}^2}{J_{0d}};\; V_{rd} = 2\frac{kT}{q}\ln\frac{J_{0r}}{J_{0d}} \quad (4)$$

Smoothing off angles between the segments is performed, if required, by summing (1) the current components.

2.1.2. Light current-voltage characteristic segment.

The light characteristic segment is obtained from a corresponding dark segment (2):

$$J_\varphi = J_g - J \quad (5)$$

where J_g is the generation current density, which proportional to the illumination intensity measured, in particular, by the sunlight concentration ratio *C; J* is the density of the external current, J_φ is the density of the forward current (in this case internal one) of a *p-n* junction. In the expression (5), the direction of J_g and J are chosen in such a way that they are positive on the load portion of the light characteristic (*J - V*). Substitution of (5) in (2) (but before J_φ substituted for *J*) gives the light voltage-current characteristic segment:

$$V_\varphi = \frac{AkT}{q}\cdot\ln\left(\frac{(J_g - J)}{J_0}+1\right) \quad (6)$$

2.2 Dark and light current-voltage characteristic of the MJSC photovoltaic part.

2.2.1. Light connectorless voltage-current characteristic segment.

The light voltage-current characteristic segment of the photovoltaic (generation) part of a MJSC is obtained by summing voltage of the segments (6) PV *p-n* junctions:

$$V_\varphi = \sum_{i=1}^{n} V_{\varphi_i} = \frac{kT}{q}\cdot\ln\left(\prod_{i=1}^{n}\left(\frac{J_{g_i} - J}{J_{0i}}+1\right)^{A_i}\right) \quad (7)$$

where *i* is the number of a PV *p-n* junction, *n* is the amount of PV *p-n* junctions. At the condition of equality of generation current densities $(J_{g1} = J_{g2} = \ldots = J_{gn}) = J_g$, and else, neglecting unity in the brackets of the expression (7) (which is valid at $V_\varphi > \frac{A_i kT}{q}$ or $(J_{gi} - J) >> J_{oi}$, we obtain $(J - V)_\varphi$. characteristic of the segment:

$$V_\varphi = \frac{AkT}{q}\cdot\ln\left(\frac{(J_g - J)}{J_0}\right) \quad (8a)$$

$$\text{or } J = J_g - J_0\exp\left(\frac{qV_\varphi}{AkT}\right) \quad (8b)$$

$$\text{where } A = A_1 + A_2 + \ldots + A_n \quad (8c)$$

$$J_0 = \sqrt[A]{J_{0_1}^{A_1}\cdot J_{0_2}^{A_2}\cdot\ldots\cdot J_{0_n}^{A_n}} \quad (8d)$$

Note that the segment (8a) has exactly the same shape as the segment of a separate PV *p-n* junction (6), but has another (resulting) value of the diode coefficient and the preexponential factor.

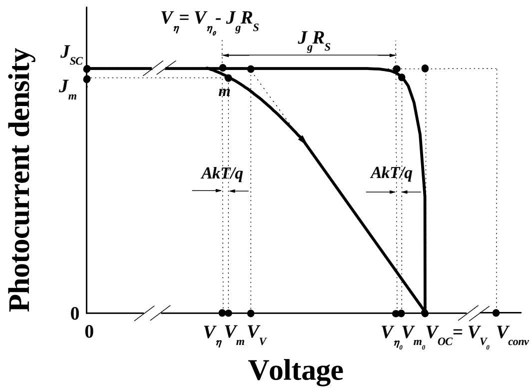

Figure 3: Schematic of the light current – voltage (load) characteristic of SCs.

2.2.2. Dark connectorless current-voltage characteristic.

The dark characteristic segment is obtained from (8a) or (8b) at a zero generation current, $J_g = 0$, and, according to (5), $J_\varphi = -J$

$$V_\varphi = \frac{AkT}{q} \cdot \ln\left(\frac{J_\varphi}{J_0} + 1\right) \quad (9a)$$

or
$$J_\varphi = J_0\left(\exp(\frac{qV_\varphi}{AkT}) - 1\right) \quad (9b)$$

Unity in brackets is added to impair a standard form to the expression (9a) and (9b). Note that the segment (9a) has the same shape as the segment of separate PV *p-n* junction (2). As a result, the whole dark current-voltage characteristic of the MJSC photovoltaic part has the same shape as the whole dark characteristic of a separate PV *p-n* junction: uninterrupted function comprised of segments. Smoothing out the angles between segments can be performed as it is done in (1) by means of summing current of the segments (9b). However, it is necessary for this that the diode coefficients of the segments would decrease with current. But this, as distinct from a separate PV *p-n* junction, is not always valid for the photovoltaic part of a MJSC.

2.2.3. Dependence of the open circuit voltage on the generated current (proportional to the sunlight concentration ratio), $V_{oc} - J_g(\propto C)$.

At the open circuit, $J_g = 0$, $V_\varphi = V_{oc}$. Then it follows from (8b) for a segment:

$$J_g = J_0 \exp\left(\frac{qV_{oc}}{AkT}\right) \quad (10)$$

The segment (10) of the $J_g - V_{oc}$ characteristic coincides with the segment (9b) of the dark $(J - V)_\varphi$ characteristic, i.e. it has alike preexponential factor J_0 and diode coefficient A values. Correspondingly, the whole $J_g - V_{oc}$ characteristic coincides with the dark $(J - V)_\varphi$ one, and also had a shape of uninterrupted function comprised of segments (p. 2.2.2).

2.3 Correlation between the optimum efficiency and the generated current (proportional to the sunlight concentration ratio), $\eta - J_g(\propto C)$.

At conventional approach [1,2], the operating voltage V_m is determined from the condition of the maximum power on the external load. To perform this, the derivative of this power is taken equal to zero, $\frac{d}{dV_\varphi}\left(J \cdot V_\varphi\right) = 0$, where the segment current J is presented by the formula (8b). Then to determine $V_{\varphi max} \equiv V_m$, it is necessary to find out the transcendent equation [7] root:

$$V_{oc} = V_m + E\ln\left(1 + \frac{V_m}{E}\right) \quad (11a)$$

or

$$\left(1 + \frac{V_m}{E}\right)\exp\left(\frac{V_m}{E}\right) = \exp\left(\frac{V_{oc}}{E}\right), \quad (11b)$$

where $E \equiv \frac{AkT}{q}$. In correspondence with (8b)

$$J_m = J_g - J_0 \exp\left(\frac{V_m}{E}\right) \quad (12)$$

or, substituting J_0 from (10) into (12) and then $\exp\left(\frac{V_{oc}}{E}\right)$ from (11b),

$$J_m = J_g \cdot \frac{V_m}{V_m + E}. \quad (13)$$

The optimum efficiency is:

$$\eta = \frac{J_m V_m}{P_{inc}} = \frac{J_g}{P_{inc}} \cdot \frac{V_m^2}{V_m + E} = \frac{V_\eta}{V_{conv}} \quad (14)$$

where P_{inc} is the power density of radiation incident on the receiving surface of a SC. At a fixed spectrum (AM0, AM1.5, laser and other), the ratio $\frac{P_{inc}}{J_g} \equiv V_{conv}$ does not depend on the illumination intensity. For this reason, the entire dependence of the efficiency on the generated current is confined in the efficiency voltage [8,9]

$$V_\eta \equiv \frac{V_m^2}{V_m + E} \quad (15)$$

By means of this quadratic (with respect to V_m) equation, the operating voltage V_m is expressed through the efficiency voltage $V_\eta \propto \eta$:

$$V_m = \frac{1}{2}\left(V_\eta + \sqrt{V_\eta(V_\eta + 4E)}\right) \quad (16)$$

The final required analytical correlation between the efficiency voltage $V_\eta(\propto \eta)$ and the generated current density $J_g(\propto C)$ is derived from the combination of (10), (11b) and (16):

$$J_g = J_0\left(1+\frac{V_\eta+\sqrt{V_\eta(V_\eta+4E)}}{2E}\right)\exp\left(\frac{V_\eta+\sqrt{V_\eta(V_\eta+4E)}}{2E}\right) \quad (17)$$

The entire $J_g(\propto C)-V_\eta(\propto \eta)$ characteristic is comprised of segments of the (17) shape and represents uninterrupted function with breaks. To smooth out the angles, summing the generation current of the segments (17) is used. However, as in the case the dark $(J-V)_\varphi$. characteristic (p.2.2.2), this is not always possible to do.

2.4 Approximate accounting for the effect of the connector part on efficiency.

2.4.1. Modified (with accounting for the connector) analytical correlation between the efficiency and generated current (proportional to the sunlight concentration ratio), $\eta - J_g(\propto C)$.

The voltage on the external load, V, is less than the voltage generated by photovoltaic *p-n* junction, V_φ, by the value equal to the voltage on the SC connecting part, V_s, $V = V_\varphi - V_s$. One may neglect this if $V_s < E \equiv \frac{AkT}{q}$.

Such a condition is fulfilled at low sunlight concentrations ($C < 10$) in the structures under investigation.

For approximate accounting for the "excess" voltage V_s, the following is supposed. First, the entire connecting part (including the tunneling p^{++}-n^{++} junctions) is simulated by one series ohmic resistance R_s. Second, it is supposed that accounting for R_s does not, practically, change the operating current J_m, which, at $V_m >> E$, is approximately equal to J_g, as follows from (13). Only the operating voltage V_m decreases and, according to (15), the efficiency voltage V_η by the value about J_gR_s. Such an assumption is based on that the shape of the connectorless (not allowing for the effect of the connector) current-voltage characteristic is close to a rectangular one (Fig. 3). It is clear from the figure that three characteristic points (rectangle vertex *v*, operating point *m* and efficiency point η) are close to each other and remain to be close in accounting for resistance. It is also seen that the voltage V_v decreases by the I_gR_s value. Hence, the efficiency voltage V_η (proportional to the efficiency $\eta = \frac{V_\eta}{V_{conv}}$) decreases by approximately the same value.

So, the approximate accounting for the effect of the connector on the efficiency lies in a drop of the connectorless efficiency voltage from the formula (12) by the J_gR_s value. In an analytical form, the modified correlation $\eta(\propto V_\eta) - C(\propto J_g)$ is following one.

$$J_g = J_0\left(1+\frac{V_{\eta 0}+\sqrt{V_{\eta 0}(V_{\eta 0}+4E)}}{2E}\right)\exp\left(\frac{V_{\eta 0}+\sqrt{V_{\eta 0}(V_{\eta 0}+4E)}}{2E}\right) \quad (18a)$$

$$V_{\eta 0} = V_\eta + J_gR_s \quad (18b)$$

where $V_{\eta 0}$ is efficiency voltage without accounting connector part. As distinct from (17), the interrelation (18a,b) between J_g and V_η attains an implicit form. Beside, a maximum of $J_{gm} \approx \frac{E}{R_s} = \frac{\left(\frac{AkT}{q}\right)}{R_s}$ appeared.

2.4.2. On a maximum of the $\eta - J_g(\propto C)$ characteristic.

In the maximum point $\frac{d\eta}{dJ_g} = 0$, hence, (formula (14)) $\frac{dV_\eta}{dJ_g} = 0$. It follows from (18b) that

$$\frac{dV_\eta}{dJ_g} = \frac{dV_{\eta 0}}{dJ_g} - R_s; \quad (19)$$

The derivative $\frac{dV_{\eta 0}}{dJ_g} = \left(\frac{dJ_g}{dV_{\eta 0}}\right)^{-1}$ is found from the equation (18a), being simplified at $V_\eta >> 4E$ (than $V_m \approx V_\eta + E$):

$$J_g \approx e \cdot J_0 \cdot \frac{V_{\eta 0}}{E} \cdot \exp\left(\frac{V_{\eta 0}}{E}\right) \quad (20)$$

where $e \approx 2.72$ is the basis of natural logarithms. As follows from (20), at using inequality $V_\eta >> 4E$, $\frac{dJ_g}{dV_{\eta 0}} \approx \frac{J_g}{E}$.

Therefore, it is seen from (19) that the generation current J_g in the efficiency maximum point $J_{gm} \approx \frac{E}{R_s}$.

3 DARK CURRENT-VOLTAGE CHARACTERISTICS (EXPERIMENT).

3.1 Dark forward current-voltage characteristic of Ge, GaAs and InGaP *p-n* junctions.

These characteristic have been obtained in the forward current density range of 10^{-11}-10^{1} A/cm^2 at room temperature. Three components of the forward current were obtained in GaAs and InGaP homo *p-n* junctions: diffusion one (A=1), recombination one (A=2) and tunneling one (A>2) (Fig. 4).

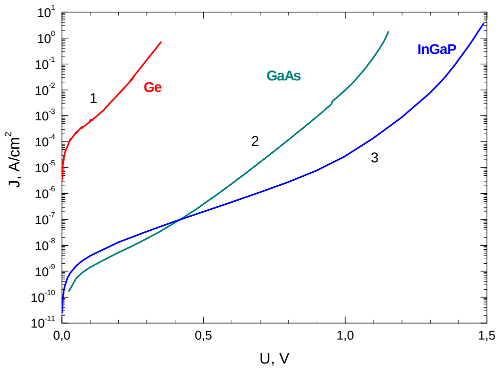

Figure 4: Experimental dark current-voltage characteristic of photovoltaic 1-Ge, 2-GaAs and 3-InGaP *p-n* junctions laced with corresponding V_{OC}-J_{SC} characteristics.

The tunneling type components revealed at the current densities lower than 10^{-6} A/cm^2 (GaAs), 10^{-5} A/cm^2 (InGaP), 10^{-4} A/cm^2 (Ge).

Values of the diffusion and recombination preexponential factors are presented in Table 1.

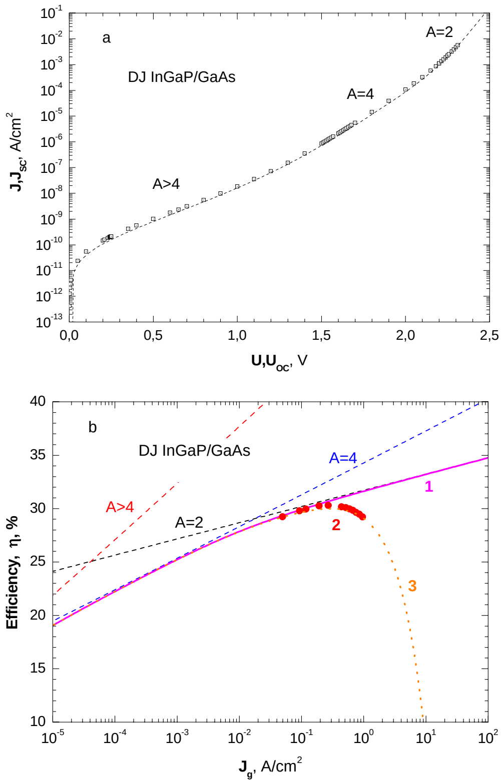

Figure 5: Characteristics of dual-junction InGaP/GaAs SC: a - experimental dark current-voltage characteristic laced with the corresponding V_{OC}-J_{SC}, where the preexponential factor $J_{0(A=4)}$=1.6·10^{-13} A/cm^2 on the segment with A=4 and the preexponential factor $J_{0(A=2)}$ = 3.1·10^{-23} A/cm^2 on the segment with A=2; b - experimental and rated dependences of the efficiency on generated current $\eta - J_g(\propto C)$: 1 – connectorless characteristic, 3 – rated $\eta - J_g(\propto C)$ characteristic by formulas (18), 2 – experimental $\eta - J_g$ dependence (circles), $J_{g(C=1)}$=13.5 mA/cm^2, AM0.

3.2 Dark forward current-voltage characteristic of the InGaP/GaAs tandems.

These characteristic have been obtained in the forward current-voltage range of (10^{-11}-10^{1}) A/cm^2 at room temperature.

The forward current-voltage characteristic of the dual-junction monolithic InGaP/GaAs tandem consists of 3 portion and is approximated by a sum of three components with the diode coefficients $A = 2$, $A = 4$ and $A > 4$ (Fig. 5). The upper portion (A=2), as follows from p.2.2.1. and 2.2.2, is formed of the diffusion portion of the GaAs and InGaP *p-n* junctions, i.e. has a pure diffusion origine. The middle portion (A=4) is formed of corresponding recombination portions and has a pure recombination origin. On the lower portion (A>4), the tunneling components has a significant contribution, at least of one homo *p-n* junction. The portion of mixed origine (A=3) (the diffusion portion of one homo *p-n* junction and the recombination portion of another one homo *p-n* junction) did not appear. This means that it short compared with the smoothing interval between the upper (A=2) and middle (A=4) portions. Besides, this indicates additionally the proximity of the current recombination-diffusion boundaries J_{rd} for InGaP and GaAs homo *p-n* junction (Table 1).

Table I:

homo *p-n* junctions	preexponential factors	
	recombination, J_{0r}	diffusion, J_{0d}
	A/cm^2	
Ge	-	(1-2) 10^{-6}
GaAs	(2-5) 10^{-11}	(1-9) 10^{-21}
InGaP	(3-7) 10^{-14}	(1-5) 10^{-26}

The preexponential factors obtained by approximation of the dark forward current-voltage characteristic by three exponents are $J_{0(A=4)}$ = (1-9)·10^{-13} A/cm^2, $J_{0(A=2)}$ = (0.5-9)·10^{-23} A/cm^2

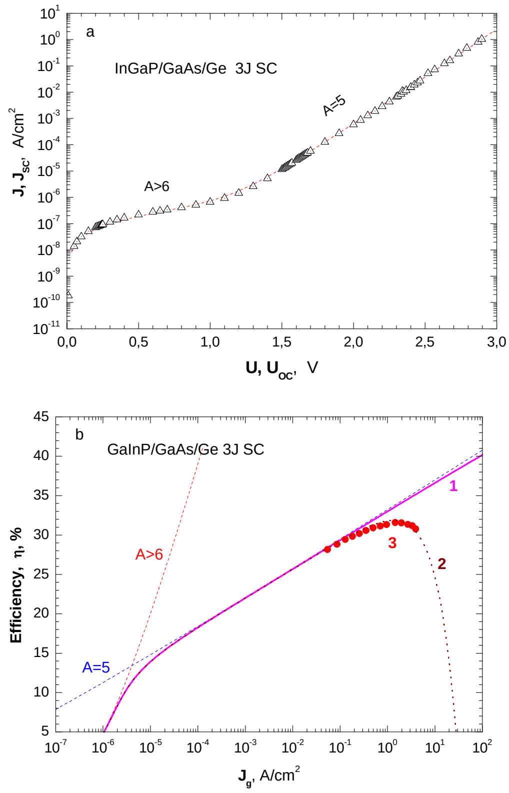

Figure 6: Characteristics of triple-junction InGaP/GaAs/Ge SC: a - experimental dark current-voltage characteristic laced with the corresponding V_{OC}-J_{SC}, where the preexponential factor $J_{0(A=5)}$ = 6·10^{-11} A/cm^2 on the segment with A=5. This segment is formed of GaAs and InGaP wideband *p-n* junctions recombination segments and Ge *p-n* junction diffusion segment; b - experimental and rated dependences of the efficiency on generated current $\eta - J_g(\propto C)$ 1 – connectorless characteristic, 2 – rated $\eta - J_g(\propto C)$ characteristic by formulas (18), 3 – experimental $\eta - J_g$ dependence (circles), $J_{g(C=1)}$=13.7 mA/cm^2, AM1.5.

3.3 Dark forward current-voltage characteristic of triple-junction InGaP/GaAs/Ge structures.

Measurements were carried out at room temperature in the current density range of $(10^{1} - 10^{-11})$ A/cm^2. The dark characteristic consist of two portions and are approximated by a sum of two exponents with diode coefficients A=5 and A>5 (Fig.6). This figure shows the dark J-V characteristic laced with the generation current-open circuit voltage characteristic $J_g - V_{oc}$, $J_g \approx J_{sc}$.

The upper portion (A=5), as follows from p.p.2.2.1. and 2.2.2., is formed of the diffusion portion of the Ge *p-n* junction, the recombination portion of the GaAs *p-n* junction and the recombination portion of the GaInP *p-n* junction, i.e. it has a mixed origin. On the lower portion (A>5), the tunneling components contribution is significant, at least in one generating *p-n* junction.

The preexponential factor on the mixed portion $J_{0(drr)} = (5 - 7)\cdot 10^{-11}$ A/cm^2. This value agrees with the formula (8c), in which the J_{0d}(Ge), J_{0r}(GaAs), J_{0r}(InGaP) values are taken from Table 1.

4 CHARACTER OF THE DEPENDENCE OF THE EFFICIENCY ON THE GENERATING CURRENT AND SUNLIGHT CONCENTRATION RATIO, $\eta - J_g(\propto C)$.

4.1 Calculation of the $J_g(\propto C) - V_\eta(\propto \eta)$ characteristic.

The experimental dark current-voltage characteristic gives a feasibility to calculate (by the formula (18) at the condition of generation current matching of photovoltaic p-n function comprising the PV part of a MJSC) and plot the generated current-efficiency voltage characteristic, J_g - V_η, for each segment. This characteristic is proportional to the sunlight concentration ratio – efficiency voltage characteristic, $C(\propto J_g) - \eta(\propto V_\eta)$.

The proportionality coefficient between J_g and C is the generation current at one sun, $J_{g,C=1}$, which is determined experimentally, since it confides at C=1 with the short circuit current, $J_{g,C=1} \approx J_{sc,C=1}$. It is necessary for such a coincidence that the condition $J_{sc}R_s < V_{oc}$ would be fulfilled, which is obeyed at C=1.

The proportionality coefficient between V_η and η is the conversion voltage, $V_{conv} = \frac{P_{inc}}{J_g}$ (p.2.3) which does not depend out the illumination intensity (at a fixed spectrum) and is usually determined at one sun (C=1), $V_{conv} = \frac{P_{inc,C=1}}{J_{g,c=1}}$. The incident radiation power densities were taken as $P_{inc,C=1} = 136.6$ mW/cm^2 (AM0) or 100 mW/cm^2 (AM1.5d).

To obtain the entire $\eta(\propto V_\eta) - C(\propto J_g)$ characteristic from segments, their generation currents were summed: $J_g = \sum_i J_{gi}$, where i is the segment index. Such a summation results is smoothing off the angels between segments. It is admissible, if the diode coefficients of the dark $(J - V)_\varphi$ characteristic decrease with increasing of the current, which is obeyed (Fig. 5,6).

4.2 Dependence efficiency – sunlight concentration ratio, $\eta(\propto V_\eta) - C(\propto J_g)$, for the InGaP/GaAs tandem.

The η – C dependence calculated by the formula (18) and plotted fits well to the experimental one at $R_s \approx 0.18$ Om·cm^2 (Fig. 5b). The coincidence indicates the validity of the following assumption and approximation done in obtained the equation (18):

1. The photovoltaic *p-n* junctions are generation current matched: $(J_{g1} = J_{g2} = \ldots J_{gn}) = J_g$.
2. The whole connecting part of a MJSC (connector) was approximated by the series ohmic resistance, R_s.
3. The efficiency voltage (proportional to the efficiency) $V_\eta(\propto \eta)$ calculated in the connectorless approximation ($R_s = 0$) was decreased by the J_gR_s value to account for the negative effect of the connector on the efficiency.

The character of the $\eta(\propto V_\eta) - C(\propto J_g)$ dependence (Fig. 5b) repeats that the dark current-voltage dependence, (Fig. 5a). Both dependencies have similar numbers of segments. Allowing for the series resistance bends the η - J_g characteristic "down" (towards smaller η) forming a maximum.

Presence of the maximum on the $\eta(\propto V_\eta) - C(\propto J_g)$ characteristic may be used for estimating the series resistance approximating the connecting part of a MJSC (connector) $R_s \approx \frac{E}{J_{g\max}}$, where $E \equiv \frac{AkT}{q}$.

4.3 Efficiency – sunlight concentration ratio dependence for a triple-junction InGaP/Ga(In)As/Ge structure.

The η – $J_g(\propto C)$ dependence calculated by the formula (18) fits well to the experimental one at $R_S = 0{,}085$ Om·cm^2 and $J_{g,C=1} = 13{,}7$ mA/cm^2. The segmental character of the dark $(J - V)_\varphi$ characteristic agrees with the $J_g(\propto C)$ - $V_\eta(\propto \eta)$ characteristic character (Fig. 6).

The coincidence indicates the validity of the assumption and approximations done in deriving the (18) equation.

The results of the analytical calculations show that, for triple-junction solar cells, one may use the model with the following three elements of an equivalent current.

1. Selected single generated current close to the generated current of a dual-junction tandem.
2. Selected series ohmic resistance approximating the entire connecting part of a multijunction solar cell.
3. Virtual (generating) *p-n* junction; the dark and "inner" (at illumination), current is summed of several exponents with diode coefficients A=3, 4, 5 and >5 (Fig. 1).

5 CONCLUSION.

In the multijunction InGaP/GaAs, InGaP/GaAs/Ge solar cells, analyzed are:

- First, correspondence between two main characteristic: dark current – voltage, J – V, and efficiency (proportional to the efficiency voltage) – sunlight concentration ratio (proportional to the generated current), $\eta(\propto V_\eta) - C(\propto J_g)$.

- Second, segmental character of these two characteristics.

The following assumption and approximations have been used:

1) segment approximation (dividing to segments) of these two characteristics,
2) generated current matching between PV *p-n* junctions comprising the PV part of a solar cell (which, strictly speaking, is not valid for InGaP/GaAs/Ge solar cells),
3) approximation of the connecting part of a SC (including tunneling *p-n* junctions) by a ohmic resistance, R_S,
4) correction (decrease) of the efficiency voltage (proportional to the efficiency) by the $J_g R_S$ value to account for the negative effect of R_S on the efficiency.

At these assumptions and approximations, an analytical correlations between the efficiency voltage, V_η, and the generated current, J_g, and, hence, between the efficiency, η, and the sunlight concentration ratio, C, has been derived. There exists a correlation between *J-V* and $\eta - C(\propto J_g)$ characteristics. At small dark and photogenerated currents, until the effect of the simulation series ohmic resistance fells upon (JR_S, $J_g R_S < AkT/q$), both these characteristics have the shape of an uninterrupted function comprised of segments with smoothed-out angels between the segments. These segments in the semilogarithmic scale are straight lines (*V-lgJ*) characteristics or almost straight line (η-*lgC*) characteristics (Fig. 5, 6).

The connectorless *J-V* characteristics of the dual-junction InGaP/GaAs solar cells have been obtained, and the segment parameters (J_0, A) have been determined, which were used for calculating and plotting the $\eta - J_g\ (\propto C)$ characteristic. The rated $\eta - J_g\ (\propto C)$ characteristics fits to the experimental ones (Fig.5) which indicates that the four assumptions and approximations done in calculating the $\eta - J_g\ (\propto C)$ characteristic are satisfactory. Moreover, such a coincidence is present for the triple-junction InGaP/GaAs/Ge solar cells, in spite of there is no generated current matching between the Ge PV *p-n* junction and the GaAs and InGaP PV *p-n* junctions.

The obtained analytical correlation between the efficiency and the generated current (proportional to the sunlight concentration ratio) is also valid for single-junction SCs (in particular, Si SCs) and other photo cells (in particular, Ge thermophotovoltaic cells), and even to larger extent. Actually, for the single-junction cell, first, there is no need for current matching and, second, the connecting part is represented by a real, but not simulating, series ohmic resistance R_S.

One of the practically useful results of the work is the following one. It has been established that, at the nonconcentrated (C=1) and weakly concentrated (C<10) sunlight in the case of GaAs and GaInP *p-n* junctions, the recombination component gives the main contribution to the dark and inner (at illumination) currents. At high (C>100) ratios in the case of Ge, GaAs, GaInP *p-n* junctions, the main contribution is given by the diffusion component. At weakened (C<1) solar illumination, the effect of the tunneling (excess) mechanism in all three PV *p-n* junctions often takes place.

6 REFERENCES

[1] V.M.Andreev, V.A. Grilikhes and V.D. Rumyantsev, Photovoltaic Conversion of Concentrated Sunlight, John Wiley & Sons Ltd., (1997)

[2] A.L. Fahrenbruch, R.H. Bube, Fundumentals of Solar Cells. Photovoltaic Solar Energy Convertion, AP, N.Y., (1983).

[3] V.S. Kalinovsky, V.V. Evstropov, N.A. Kaluzhniy, V.M. Lantratov, S.A. Mintairov and V.M. Andreev, 23rd European Photovoltaic Solar Energy Conference, Valencia, Spain (2007).

[4] L. Esaki, Solid State Physics in Electronics and Telecomunications, Proc. Int. Conf., Brussels, (1958), v.1, Semiconductors, pt. I, N.Y. (1960), 514.

[5] A.R. Riben, D.L. Feucht, Solid State Electron., v. 9,(1966), 1055.

[6] V.M. Andreev, V.V. Evstropov, V.S. Kalinovsky, V.M. Lantratov, and V.P. Khvostikov, Semiconductors, 2009, Vol. 43, No. 5, 644.

[7] W. Shockley, H.J. Quesser, J. Appl. Phys., v. 32, (1961), 510

[8] M.Wolf J. Vac. Technol., 12, (1975), 984

[9] C.H. Henry. J Appl. Phys. 51(3), (1980), 4494